MOEM

Modern Electronic Materials 2022; 8(4): 165–171
DOI 10.3897/j.moem.8.4.100756

Research Article

Correct determination of electron concentration in *n*-GaSb by electrical measurements

Yuri N. Parkhomenko[1], Aleksandr G. Belov[1], Elena V. Molodtsova[1], Roman Yu. Kozlov[1], Svetlana S. Kormilitsina[1], Eugene O. Zhuravlev[1]

1 *Federal State Research and Development Institute of Rare Metal Industry (Giredmet JSC), 2-1 Elektrodnaya Str., Moscow 111524, Russian Federation*

Corresponding author: Aleksandr G. Belov (iadenisov@giredmet.ru)

Received 17 November 2022 ♦ **Accepted** 12 December 2022 ♦ **Published** 19 December 2022

Citation: Parkhomenko YuN, Belov AG, Molodtsova EV, Kozlov RYu, Kormilitsina SS, Zhuravlev EO (2022) Correct determination of electron concentration in *n*-GaSb by electrical measurements. *Modern Electronic Materials* 8(4): 165–171. https://doi.org/10.3897/j.moem.8.4.100756

Abstract

The concentrations of conduction electrons in *n*-GaSb at 295 and 77 K have been calculated taking into account the non-parabolic deviation of the conduction band shape. We show that at $T = 295$ K the concentration of heavy electrons in the *L*-valley of the conduction band is higher than the concentration of light electrons in the Γ-valley. On the contrary, at $T = 77$ K the conduction electrons are mostly concentrated in the Γ-valley.

Hall data for tellurium doped CZ *n*-GaSb specimens have been reported. Analysis of experimental data for $T = 295$ K requires the existence of two types of electrons be taken into account (the light and the heavy ones), the concentrations of which cannot be determined. The apparent increase in the electron concentration with a decrease in the temperature from 295 to 77 K is not true. The concentration of conduction electrons at $T = 77$ K can be measured correctly with the Hall method.

Keywords

concentration of conduction electrons, gallium antimonide, light and heavy electrons

1. Introduction

Giredmet JSC has been for many years developing contactless nondestructive methods for room temperature measurement of free carrier concentration in heavily doped semiconductors. Free carrier concentration measurement includes taking far infrared reflection spectra of test specimens and determination of characteristic frequencies by mathematical processing of the reflection spectra. Studies have been conducted for $Pb_{1-x}Sn_xTe$ [1], $Cd_xHg_{1-x}Te$ [2], *n*-GaAs [3] and *n*-InAs [4]. Optically measured free carrier concentrations are typically compared against electrical measurement data.

This work is a continuation of our earlier series of studies [1–4] while it does not deal directly with optical measurements which are a subject of a separate study. Unlike for the above-listed semiconductor compounds, the treatise of room temperature electrical measurement data for *n*-GaSb is a complex task by itself and requires a special approach which will be described below in this work. The results obtained in this study will be further used for the calculations of optical parameters of *n*-GaSb.

The band structure and electrical properties of *n*-GaSb have been well studied for a long time (see e.g. [5–17] and overviews [18, 19]). However, there are a number of persistent questions relating to the treatise of electrical measurement data. For example, there is no explanation of the fact that the conduction electron concentration allegedly increases as the temperature decreases from room to liquid nitrogen one [20, 21].

Noteworthy, the concentration and mobility of electrons are calculated from Hall data using simple formulas in the assumption that *n*-GaSb specimens contain only one type of electrons. We will show below that this approach is not fully justified and needs correction.

The aim of this work is to calculate the concentrations and effective masses of conduction electrons in n-GaSb at 295 and 77 K.

2. Theoretical calculations

It is well known that the conduction band of GaSb has several valleys [12–18]. Figure 1 shows the band structure of GaSb as reported earlier [22].

The cited work also reported formulas describing the temperature dependences of the energy gaps E_g and EL:

$$E_g = 0.813 - \frac{3.78 \cdot 10^{-4} T^2}{T + 94}; \quad (1)$$

$$E_L = 0.902 - \frac{3.97 \cdot 10^{-4} T^2}{T + 94}, \quad (2)$$

where T is the absolute temperature.

Using Eqs. (1) and (2) one can calculate the energy gaps for 295 and 88 K:

– for $T = 295$ K:

$E_{g295} = 0.728$ eV; $E_{L295} = 0.813$ eV;

$\Delta E_{295} = E_{L295} - E_{g295} = 0.085$ eV = 85 meV;

– for $T = 77$ K:

$E_{g77} = 0.800$ eV; $E_{L77} = 0.888$ eV;

$\Delta E_{77} = E_{L77} - E_{g77} = 0.088$ eV = 88 meV.

It can be seen from these data that the gap ΔE is almost temperature-independent.

Taking into account that for $T = 295$ K, $kT = 25.4$ meV ($k = 1.38 \cdot 10^{-16}$ erg/deg is the Boltzmann constant) and for $T = 77$ K, $kT = 6.63$ meV, we obtain that $\Delta E_{295}/kT = 3.35$ and $\Delta E_{77}/kT = 13.3$. It is therefore reasonable to expect that at the LN temperature all the conduction electrons will be concentrated in the Γ-valley and at room temperature, they will be distributed between the

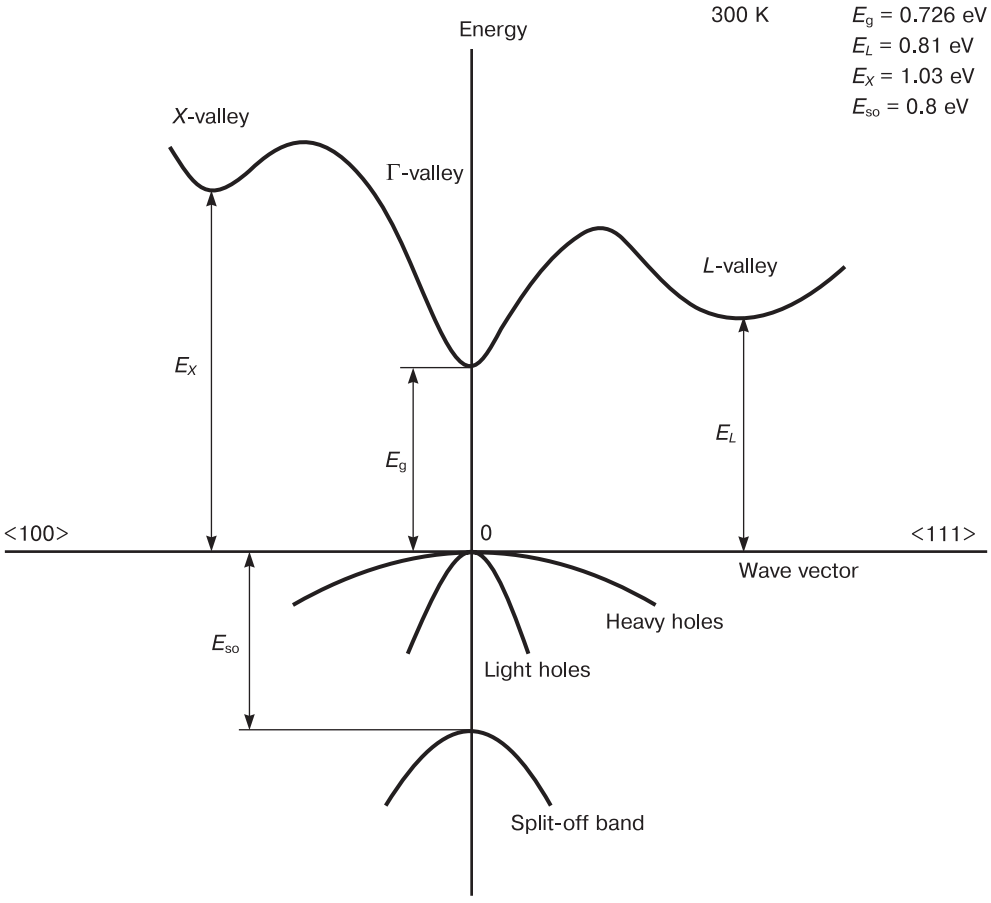

Figure 1. Band structure of GaSb [22]

Γ- and the *L*-valleys. The calculations below confirm this assumption.

We consider the statistics for conduction electrons in *n*-GaSb at room temperature (T = 295 K). The Γ-valley of the conduction band is described by the Kane dispersion law [23], with the following relations being true ([24], Appendix A):

$$n_1 = \frac{\sqrt{3}}{2\sqrt{2}\pi^2}\frac{\left(kTE_g\right)^{3/2}}{P_{cv}^3}\,{}^0L_0^{3/2}(\eta,\beta); \tag{3}$$

$$\frac{m_1}{m_0} = \frac{3\hbar^2 E_g}{4P_{cv}^2}\frac{{}^0L_0^{3/2}(\eta,\beta)}{{}^0L_{-1}^{3/2}(\eta,\beta)}\frac{1}{m_0}; \tag{4}$$

where n_1 and m_1 are the concentration and effective mass of electrons in the Γ-valley, respectively, $m_0 = 9.11\cdot10^{-28}$ g is the mass of a free electron, P_{cv} = $8{,}7\cdot10^{-8}$ eV · cm [25] is the matrix element of interaction between the conduction band and the light hole band (in the Γ-Brillouin zone point) and $\hbar = h/2\pi$, where $h = 6.62\cdot10^{-27}$ erg · s is the Planck constant. It is assumed that the parameter P_{cv} does not depend on energy and temperature [25] since this form significantly simplifies the calculations.

Equations (3) and (4) use two-parameter Fermi integrals:

$${}^mL_k^n(\eta,\beta) = \int_0^\infty\left(-\frac{\partial f_0}{\partial x}\right)\frac{x^m\left(x+\beta x^2\right)^n}{\left(1+2\beta x\right)^k}\,dx, \tag{5}$$

where

$$f_0 = [1 + \exp(x - \eta)]^{-1}, \tag{6}$$

$\eta = E_F/kT$ is the reduced Fermi level (counted upward from the conduction band bottom in the point Γ); $\beta = kT/E_g$ is the parameter describing the non-parabolic deviation of the Γ-valley in the conduction band.

Unlike the Γ-valley, the *L*-valley of the conduction band can be considered parabolic. It consists of four rotation ellipsoids. The longitudinal effective mass is $m_{2l} = 0.95m_0$, the transverse one being $m_{2t} = 0.11m_0$ [22], i.e., the anisotropy coefficient is $K_1 = m_{2l}/m_{2t} = 8.64$. Accordingly, the effective mass of the density of states (per one ellipsoid) is as follows:

$$m_d^{(1)} = \sqrt[3]{m_t^2 m_l} = m_t K_1^{1/3} = 0.2257m_0. \tag{7}$$

The concentration of electrons in the *L*-band n_2 is described by the following relationship:

$$n_2 = M\frac{8\pi}{3h^3}\left(2m_d^{(1)}kT\right)^{3/2}F_{3/2}(\eta-3.35), \tag{8}$$

Here $M = 4$ is the number of ellipsoids in the *L*-valley and $F_{3/2}(\eta)$ is the single-parameter Fermi integral.

The integral ${}^0L_0{}^{3/2}(\eta, \beta)$ transforms to $F_{3/2}(\eta)$ at $\beta \to 0$, i.e., if the non-parabolic deviation of the band shape can be ignored. The argument of the integral $F_{3/2}$ in Eq. (8) is $(\eta - 3.35)$ because the *L*-band is located $3.35kT$ above the Γ-band.

As a result, Eqs. (3), (4) and (8) transform as follows for T = 295 K:

$$n_1 = 2.376\cdot10^{17}\cdot{}^0L_0{}^{3/2}(\eta, 0.0349); \tag{9}$$

$$\frac{m_1}{m_0} = 0.0550\frac{{}^0L_0^{3/2}(\eta,0.0349)}{{}^0L_{-1}^{3/2}(\eta,0.0349)}; \tag{10}$$

$$n_2 = 7.900\cdot10^{18}\cdot F_{3/2}(\eta - 3.35). \tag{11}$$

Then, substituting η in the range (–4,0 ÷ +4,0) into Eqs. (9)–(11) one can calculate the above-listed parameters as follows (Table 1).

As can be seen from Table 1 the n_2 values are always greater than n_1, this difference increasing with an increase in the reduced Fermi level. For example, for η = –4, $n_1 \approx n_2$, whereas for η = 2, $n_2/n_1 = 2.34$ (see Table 1). In other words in the range $n_1 \sim 10^{18}$ cm^{-3} most conduction electrons are concentrated in the *L*-band.

We now consider the statistics for electrons at the liquid nitrogen temperature (T = 77 K). Taking into account that $\beta = kT/E_g = 0.00829$ and $\Delta E/kT = 13.3$, Eqs. (3), (4) and (8) can be transformed as follows:

$$n_1 = 3.649\cdot10^{16}\cdot{}^0L_0{}^{3/2}(\eta, 0.00829); \tag{12}$$

$$\frac{m_1}{m_0} = 0.064\frac{{}^0L_0^{3/2}(\eta,0.00829)}{{}^0L_{-1}^{3/2}(\eta,0.00829)}; \tag{13}$$

$$n_2 = 1.053\cdot10^{18}\cdot F_{3/2}(\eta - 13.3). \tag{14}$$

The results of calculations with Eqs. (12)–(14) are summarized in Table 2.

The value η = +13.3 corresponds to the Fermi level position at the bottom of the *L*-valley in the conduction band.

It can be seen from Table 2 that unlike for T = 295 K, n_1 is always greater than n_2 (conduction electrons are mostly concentrated in the Γ-valley). Only for $n_1 \approx 2\cdot10^{18}$ cm^{-3} the n_2 values prove to be of the same order of magnitude.

The concentration and mobility of electrons in *n*-GaSb are usually calculated with the following formulas (it is assumed that there are electrons of only one type):

$$\rho = (en\mu)^{-1}; \tag{15}$$

$$|R| = \frac{1}{ne}; \tag{16}$$

$$\mu = \frac{|R|}{\rho}. \tag{17}$$

Here ρ is the electrical resistivity (Ohm · cm), R is the Hall coefficient (cm^3/C); μ is the electron mobility (cm^2/(V · s)); $e = 1.6\cdot10^{-19}$ C is the electron charge (taken by absolute value).

Table 1. Calculated parameters for $T = 295$ K

E_F/kT	${}^0L_0{}^{3/2}$ (η, 0.0349)	${}^0L_{-1}{}^{3/2}$ (η, 0.0349)	n_1 (cm^{-3})	m_1/m_0	$F_{3/2}$ (η – 3.35)	n_2 (cm^{-3})
–4.0	0.02746	0.02341	$6.525 \cdot 10^{15}$	0.0645	$8.540 \cdot 10^{-4}$	$6.747 \cdot 10^{15}$
–3.5	0.04510	0.03843	$1.072 \cdot 10^{16}$	0.0646	$1.408 \cdot 10^{-3}$	$1.112 \cdot 10^{16}$
–3.0	0.07389	0.06293	$1.756 \cdot 10^{16}$	0.0646	$2.321 \cdot 10^{-3}$	$1.833 \cdot 10^{16}$
–2.5	0.1206	0.1026	$2.865 \cdot 10^{16}$	0.0646	$3.825 \cdot 10^{-3}$	$3.021 \cdot 10^{16}$
–2.0	0.1956	0.1662	$4.647 \cdot 10^{16}$	0.0647	$6.301 \cdot 10^{-3}$	$4.978 \cdot 10^{16}$
–1.5	0.3143	0.2665	$7.468 \cdot 10^{16}$	0.0649	$1.037 \cdot 10^{-2}$	$8.192 \cdot 10^{16}$
–1.0	0.4879	0.4209	$1.188 \cdot 10^{17}$	0.0651	$1.708 \cdot 10^{-2}$	$1.349 \cdot 10^{17}$
–0.5	0.7738	0.6512	$1.839 \cdot 10^{17}$	0.0654	$2.808 \cdot 10^{-2}$	$2.218 \cdot 10^{17}$
0	1.173	0.9805	$2.787 \cdot 10^{17}$	0.0658	$4.607 \cdot 10^{-2}$	$3.640 \cdot 10^{17}$
0.5	1.725	1.430	$4.098 \cdot 10^{17}$	0.0664	$7.537 \cdot 10^{-2}$	$5.954 \cdot 10^{17}$
1.0	2.455	2.012	$5.833 \cdot 10^{17}$	0.0671	0.1227	$9.693 \cdot 10^{17}$
1.5	3.379	2.732	$8.028 \cdot 10^{17}$	0.0680	0.1983	$1.566 \cdot 10^{18}$
2.0	4.506	3.588	$1.071 \cdot 10^{18}$	0.0691	0.3169	$2.504 \cdot 10^{18}$
3.0	7.378	5.669	$1.753 \cdot 10^{18}$	0.0716	0.7655	$6.047 \cdot 10^{18}$
4.0	11.07	8.178	$2.631 \cdot 10^{18}$	0.0745	1.653	$1.306 \cdot 10^{19}$

Table 2. Calculated parameters for *n*-GaSb at $T = 77$ K

$\eta = E_F/kT$	${}^0L_0{}^{3/2}$ (η, 0.00829)	${}^0L_{-1}{}^{3/2}$ (η, 0.00829)	n_1 (cm^{-3})	m_1/m_0	$F_{3/2}$ (η – 13,3)	n_2 (cm^{-3})
+2	3.927	3.702	$1.433 \cdot 10^{17}$	0.0648	$1.645 \cdot 10^{-5}$	$1.732 \cdot 10^{13}$
+5	12.63	11.51	$4.609 \cdot 10^{17}$	0.0663	$3.303 \cdot 10^{-4}$	$3.478 \cdot 10^{14}$
+8	25.58	22.39	$9.335 \cdot 10^{17}$	0.0690	$6.624 \cdot 10^{-3}$	$6.975 \cdot 10^{15}$
+10	36.28	30.91	$1.324 \cdot 10^{18}$	0.0709	0.04840	$5.097 \cdot 10^{16}$
+13.3	57.38	46.78	$2.094 \cdot 10^{18}$	0.0741	1.017	$1.071 \cdot 10^{18}$

This approach is justified at low temperatures ($T = 77$ K) but is absolutely erroneous for $T = 295$ K when the conduction electrons are mostly concentrated in the *L*-valley (Table 1). In this case (two types of conduction electrons) Eq. (16) describing the Hall coefficient should be replaced for a more complex one:

$$|R| = \frac{1}{e}\frac{n_1\mu_1^2 + n_2\mu_2^2}{(n_1\mu_1 + n_2\mu_2)^2}, \tag{18}$$

where μ_1 and μ_2 are the electron mobilities in the Γ- and *L*-valleys, respectively.

Introducing the dimensionless parameter $b = \mu_1/\mu_2$ describing the relation of the electron mobilities in the Γ- and *L*-valleys of the conduction band, one can transform Eq. (18) as follows:

$$|R| = \frac{1}{e}\frac{n_1 b^2 + n_2}{(n_1 b + n_2)^2}, \tag{19}$$

The values n_1 and n_2 are interrelated (see Eqs. (3) and (8)) but the parameter *b* is unknown. In other words the use of Eq. (16) for calculations at $T = 295$ K instead of the correct formula (Eq. (19)) yields some "effective" electron concentration which is only close to n_1 and n_2 by the order of magnitude.

3. Experimental results and discussion

We studied *n*-GaSb specimens cut from ingots grown with the upgraded Czochralski method. 6N purity raw Ga and Sb components with the Te doping impurity were charged into a quartz filtering crucible installed inside the working crucible in the growth chamber. The GaSb compound was synthesized in the filtering crucible in a hydrogen flow at ~800 °C. The melt was then filtered into the working crucible and the temperature was reduced to 714 °C. The single crystal was grown from a [100] seed and annealed in the heater zone. Annealing mode was experimentally selected.

Electrical measurements were conducted for cylindrical reference wafers cut from the top and bottom sections of the single crystal, grounded with M14 powder and etch-polished for damaged layer removal. The wafers were then cut into 10–15 mm sized specimens. The

Table 3. Results of electrica measurements

Specimen #	d (mm)	T (K)	ρ (Ohm · cm)	$\|R\|$ (cm^3/C)	$n = 1/(\|R\|e)$ (cm^{-3})	$\mu = \|R\|/\rho$ ($cm^2/(V \cdot s)$)	n_{77}/n_{295}
1	0.55	295	$6.20 \cdot 10^{-3}$	18.1	$3.45 \cdot 10^{17}$	$2.9 \cdot 10^3$	1.74
		77	$2.02 \cdot 10^{-3}$	10.4	$6.01 \cdot 10^{17}$	$5.2 \cdot 10^3$	
2	1.99	295	$5.26 \cdot 10^{-3}$	14.9	$4.19 \cdot 10^{17}$	$2.8 \cdot 10^3$	1.65
		77	$1.72 \cdot 10^{-3}$	8.66	$7.23 \cdot 10^{17}$	$5.0 \cdot 10^3$	
3	0.45	295	$4.56 \cdot 10^{-3}$	13.9	$4.50 \cdot 10^{17}$	$3.1 \cdot 10^3$	1.65
		77	$1.36 \cdot 10^{-3}$	8.41	$7.43 \cdot 10^{17}$	$6.2 \cdot 10^3$	
4	2.12	295	$4.75 \cdot 10^{-3}$	13.6	$4.60 \cdot 10^{17}$	$2.9 \cdot 10^3$	1.68
		77	$1.51 \cdot 10^{-3}$	8.07	$7.74 \cdot 10^{17}$	$5.3 \cdot 10^3$	
5	0.50	295	$3.04 \cdot 10^{-3}$	8.10	$7.72 \cdot 10^{17}$	$2.7 \cdot 10^3$	1.37
		77	$9.13 \cdot 10^{-4}$	5.89	$1.06 \cdot 10^{18}$	$6.5 \cdot 10^3$	
6	0.94	295	$3.16 \cdot 10^{-3}$	7.47	$8.37 \cdot 10^{17}$	$2.4 \cdot 10^3$	1.46
		77	$9.53 \cdot 10^{-4}$	5.11	$1.22 \cdot 10^{18}$	$5.4 \cdot 10^3$	
7	1.36	295	$2.32 \cdot 10^{-3}$	6.09	$1.03 \cdot 10^{18}$	$2.6 \cdot 10^3$	1.25
		77	$7.17 \cdot 10^{-4}$	4.83	$1.29 \cdot 10^{18}$	$6.7 \cdot 10^3$	
8	2.04	295	$1.71 \cdot 10^{-3}$	4.46	$1.40 \cdot 10^{18}$	$2.6 \cdot 10^3$	1.10
		77	$5.68 \cdot 10^{-4}$	4.07	$1.54 \cdot 10^{18}$	$7.2 \cdot 10^3$	

specimen thickness was $d = 0.55$–2.04 mm (Table 3). The contacts were flux-soldered to flat specimen surfaces. The contact material was indium.

Two test specimens were placed at opposite sides of a two-side specimen holder, and the conductor wires were soldered to the respective contact pads of the specimen holder. The specimen holder with the specimens was placed into a foam plastic cryostat installed between the poles of an electric magnet. The cryostat was filled with liquid nitrogen to a level to cover the specimens. The measurements were run using the conventional four-probe setup (the Van der Pau method).

The electrical resistivity of the specimens was measured without a magnetic field, and the Hall measurements were run at the magnetic field induction $B = 0.5$ T, the current through the specimen being $I_{spec} = 200$ mA.

The results of the electrical measurements for the n-GaSb specimens at 295 and 77 K are summarized in Table 3. The specimens are presented in order of increasing the electron concentration at $T = 77$ K.

As can be seen from Table 3, the values $1/|R|e$ for $T = 77$ K are always greater than those for $T = 295$ K, the n_{77}/n_{295} ratio decreasing with an increase in n_{77}. It was noted above that only the data for $T = 77$ K can be considered authentic, whereas correct treatise of the data for $T = 295$ K is impossible.

Using Tables 1 and 3 one can approximately evaluate the values n_1 и n_2 for $T = 295$ K if n_1 for $T = 77$ K is known. For example for Specimen 7 (Table 3), $n_{77} = 1.29 \cdot 10^{18}$ cm^{-3}, and $n = 1/|R|e$ for $T = 295$ K is $1.03 \cdot 10^{18}$ cm^{-3}. Accepting that n_1 remains the same at $T = 295$ K, one can conclude from Table 1 that for $E_F/kT = +2$, $n_1 \approx 1.07 \cdot 10^{18}$ cm^{-3} and $n_2 \approx 2.50 \cdot 10^{18}$ cm^{-3}. Accordingly, $(n_1 + n_2)_{295} \approx 3.57 \cdot 10^{18}$ cm^{-3}, which is *a priori* greater than $n = 1/(Re)_{295} = 1.29 \cdot 10^{18}$ cm^{-3}. Thus the apparent increase in the electron concentration upon specimen cooling is actually not the case.

The conductivity and Hall effect were analyzed as a function of temperature and pressure earlier [6, 7]. The experimental data were treated using a theoretical model that implied a number of questionable simplifications. For example, Kane's non-parabolic deviation of the Γ-band shape was not taken into account, and the effective mass of electrons in this band was considered temperature- and energy-independent and accepted to be $m_1 = 0.047m_0$ which is considerably less than the calculation data presented in Tables 1 and 2.

Furthermore, the overall electron concentration in the Γ- and L-bands was also considered to be temperature-independent and accepted equal to the concentration of the donor impurity N_D introduced into the specimen which is completely ionized in the entire experimental temperature range [6, 7]. Even complying with this questionable assumption one should admit the lack of clarity as to how to determine N_D. It was shown [26] that the doping impurity concentration in GaSb increases with its content in the charge until a certain threshold, exceeding which it sees a plateau. Therefore, in order to deliver a correct treatise of Hall data one should know the concentration of tellurium in the test specimen, which the authors of the cited study did not know [6, 7]. The overall electron concentration is not a constant parameter and is temperature dependent [27].

Finally the value $b = 6$ was obtained for the mobility ratio over the entire 77–300 K range. This result can hardly be considered plausible taking into account the above

line of reasoning. On the contrary, it was affirmed [27] that the parameter b depends on temperature and varies in a range of 5–21, while the value $b = 16.7$ was reported elsewhere [28].

The first estimate $m_1 = 0.047m_0$ was obtained [5] for the temperatures 1.5 and 4.2 K. Later on these values of close ones were used by many authors, i.e., from $0.039m_0$ [9] to $0.052m_0$ [8, 28]. The energy and temperature dependences of the effective mass of electrons in the Γ-band were still ignored. Kane model calculations [23] (see above) yield completely different results. As can be seen from Tables 1 and 2 the smallest value of this parameter is $0.0645m_0$ at $T = 295$ K and $0.0648m_0$ at $T = 77$ K, i.e., the calculated m_1 are noticeably greater than the above experimental ones. This fact causes changes to the entire free carrier statistics. However, this question requires a separate study.

It was reported [29] that the energy parameter

$$C = \frac{2m_0 P_{cv}^2}{3\hbar^2}$$

employed in the Kane theory [23] is $C = 20/3$ eV which corresponds to $P_{cv} = 8.73 \cdot 10^{-8}$ eV · cm which is close to the value $P_{cv} = 8.7 \cdot 10^{-8}$ eV · cm [25] accepted by us for calculations (Eqs. (3)–(4)). It was noted above that the parameter P_{cv} is assumed to be energy- and temperature-independent. This opinion is confronted by other authors [30] arguing that the energy parameter C is not constant and varies in a range of 5.999–6.109 for energies of 0.70–0.813 eV, i.e., the parameter P_{cv} is $(8.28–8.35) \cdot 10^{-8}$ eV · cm.

We plan a special study to determine the parameter b for each specimen at room temperature by comparing between data of optical and electrical measurements. The calculations presented in this work will be used in that study.

4. Conclusion

Statistics of conduction electrons in the Γ- (n_1) and L- valleys (n_2) of the conduction band of GaSb at 295 and 77 K were calculated.

We show that at $T = 295$ K the electron concentration in the L-valley is greater than that in the Γ-valley. One should therefore take into account the existence of these two types of electrons when treating data of electrical measurements. Correct determination of n_1 and n_2 is impossible in this case.

We also show that at $T = 77$ K almost all the electrons are concentrated in the Γ-band. Analysis of Hall data allows definitive evaluation of the concentration and mobility of electrons.

Room and LN temperature electrical measurements were carried out for a series of n-GaSb specimens. The electron concentrations in the Γ- and L-bands at $T = 295$ K were evaluated and it was shown that the apparent increase in the electron concentration with a decrease in temperature is actually not true.

References

1. Belogorokhov A.I., Belov A.G., Petrovitch P.L., Rashevskaya E.P. Determination of the concentration of free charge carriers in $Pb_{1-x}Sn_xTe$ taking into account the damping of plasma oscillations. *Optics and Spectroscopy*, 1987; 63(6): 1293–1296. (In Russ.)
2. Belogorokhov A.I. Belogorokhova L.I., Belov A.G., Rashevskaya E.P. Plasma resonance of free charge carriers and estimation of some parameters of the band structure of the material $Cd_xHg_{1-x}Te$. *Semiconductors*. 1991; 25(7): 1196–1203. (In Russ)
3. Yugova T.G., Belov A.G., Kanevskii V.E., Kladova E.I., Knyazev S.N., Comparison between optical and electrophysical data on free electron concentration in tellurium doped *n*-GaAs samples. *Modern Electronic Materials*. 2020; 6(3): 85–89. https://doi.org/10.3897/j.moem.6.3.64492
4. Yugova T.G., Belov A.G., Kanevskii V.E., Kladova E.I., Knyasev S.N., Parfent'eva I.B. Comparison between results of optical and electrical measurements of free electron concentration in *n*-InAs specimens. *Modern Electronic Materials*. 2021; 7(3): 79–84. https://doi.org/10.3897/j.moem.7.3.76700
5. Zwerdling S., Lax B., Button K.J., Roth L.M. Oscillatory magneto-absorption in gallium antimonide JA-1149. *Journal of Physics and Chemistry of Solids*. 1959; 9(3-4): 320–324.
6. Sagar A. Experimental investigation of conduction band of GaSb. *Physical Review Journals Archive*. 1960; 117(1): 93–100. https: //doi.org/10.1103/PhysRev.117.93
7. Strauss A.J. Electrical properties of *n*-type GaSb. *Physical Review Journals Archive*. 1961; 121(4): 1087–1090. https://doi.org/10.1103/PhysRev.121.1087
8. Sun R.-Y., Becker W.M. Band inversion and transport properties of L minima in *n*-GaSb(Te). *Physical Review B*. 1974; 10: 3436–3450. https://doi.org/10.1103/PhysRevB.10.3436
9. Kourkoutas C.D., Bekris P.D., Papaioannou G.J., Euthymiou P.C. Transport parameters of *n*-type GaSb. *Solid State Communications*. 1984; 49(11): 1071–1075. https://doi.org/10.1016/0038-1098(84)90426-5
10. Johnson G.R., Cavenett B.C., Kerr T.M., Kirby P.B., Wood C.E.C. Optical, Hall and cyclotron resonance measurements of GaSb grown by molecular beam epitaxy. *Semiconductor Science and Technology*. 1988; 3(12): 1157–1165. https://doi.org/10.1088/0268-1242/3/12/002
11. Lee M.E., Poole I., Truscott W.S., Cleverly I.R., Rohlfing D.M. A detailed Hall-effect analysis of sulfur-doped gallium antimonide grown by molecular-beam epitaxy. *Journal of Applied Physics*. 1990; 68(1): 131–137. https://doi.org/10.1063/1.347098

12. Chin V.W.L. Electron mobility in GaSb. *Solid-State Electronics*. 1995; 38(1): 59–67. https://doi.org/10.1016/0038-1101(94)E0063-K
13. Dmitriev A.P., Mikhailova M.P., Yassievich I.N. Impact ionization in $A^{III}B^{V}$ semiconductors in high electric fields. *Physica Status Solidi (b)*. 1987; 140: 9–37. https://doi.org/10.1002/PSSB.2221400102
14. Gorelik S.S., Dashevskii M.Ya. Materials science of semiconductors and dielectrics. Moscow: MISiS; 2003. 480 p. (In Russ.)
15. Maslar J.E., Hurst W.S., Wang C.A. Spectroscopic determination of electron concentration in *n*-type GaAs. *Journal of Applied Physics*. 2008; 104(10): 103521–103527. https://doi.org/10.1063/1.3021159
16. Mitchel W.C., Elhamri S., Haugan H.J., Berney R., Sin Mou, Brown G.J. Electrical properties of *n*-type GaSb substrates and *p*-type GaSb buffer layers for InAs/InGaSb superlattice infrared detectors. *AIP Advances*. 2015; 5(9): 097219. https://doi.org/10.1063/1.4932208
17. Curran A., Gity F., Gocalinska A., Mura E., Nagle R.E., Schmidt M., Sheehan B., Pelucchi E., O'Dwyer C., Hurley P.K. High hole mobility polycrystalline GaSb thin films. *Crystals*. 2021; 11(11): 1348–1357. https://doi.org/10.3390/cryst11111348
18. Dutta P.S., Bhat H.L., Kumar V. The physics and technology of gallium antimonide: An emerging optoelectronic material. *Journal of Applied Physics*. 1997; 81(9): 5821–5870. https://doi.org/10.1063/1.36535610.1063/1.365356
19. Vurgaftman I., Meyer J.R., Ram-Mohan L.R. Band parameters for III-V compound semiconductors and their alloys. *Journal of Applied Physics*. 2001; 89(11): 5815–5875. https://doi.org/10.1063/1.1368156
20. Kunitsyn A.E., Chaldyshev V.V., Mil'vidskaya A.G., Mil'vidskiĭ M.G. Properties of tellurium-doped gallium antimonide single crystals grown from nonstoichiometric melt. *Semiconductors*. 1997; 31(8): 806–808. (In Russ.)
21. Khvostikov V.P., Sorokina S.V., Potapovich N.S., Khvostikova O.A., Vlasov A.S., Rakova E.P., Andreev V.M. Examination of properties of epitaxial and bulk gallium antimonide. *Semiconductors*. 2008; 42(10): 1179–1186. (In Russ.)
22. New semiconductor materials. Biology systems. Characteristics and properties. Band structure and carrier concentration of gallium antimonide (GaSb). https://www.ioffe.ru/SVA/NSM/Semicond/GaSb/bandstr.html (accessed on 20.03.2022).
23. Kane E.O. Band structure of indium antimonide. *Journal of Physics and Chemistry of Solids*. 1957; 1(4): 249–261. https://doi.org/10.1016/0022-3697 (57)90013-6
24. Stil'bans L.S., ed. Ravich Yu.I., Efimova B.A., Smirnov I.A. Methods for studying semiconductors as applied to lead chalcogenides PbTe, PbSe, PbS. Moscow: Nauka; 1968. 384 p. (In Russ.)
25. Madelung O. Physics of III-V compounds. J. Wiley; 1964. 409 p. (Russ. Transl.: Madelung O. Fizika poluprovodnikovykh soedinenii elementov III-V grupp. Moscow: Mir; 1967. 480 p.)
26. Glazov V.M., Glagoleva N.N., Gryazeva N.L. Concentration dependence of the number of charge carriers with simple and complex doping of gallium antimonide and its relationship with the solubility limit. *Semiconductors*. 1976; 10(5): 882–888. (In Russ.)
27. Harland H.B., Woolley J.C. Conduction band of GaSb. *Canadian Journal of Physics*. 1966; 44(11): 2715–2728. https://doi.org/10.1139/p66-221
28. Becker W.M., Ramdas A.K., Fan H.Y. Energy band structure of gallium antimonide. *Journal of Applied Physics*. 1961; 32(10): 2094–2102. https://doi.org/10.1063/1.1777023
29. Wolf H.F. Semiconductors. NY, USA: Wiley-Interscience; 1971. 552 p.
30. Sharma A.C., Ravindra N.M., Auluck S., Srivastava V.K. Temperature-dependent effective masses in III-V compound semiconductors. *Physica Status Solidi (b)*. 1983; 120(2): 715–721. https://doi.org/10.1002/pssb.2221200231